Sensitivity of Carbon Anode Baking Model Outputs to Kinetic Parameters Describing Pitch Pyrolysis

ARTICLE *in* INDUSTRIAL & ENGINEERING CHEMISTRY RESEARCH · MARCH 2013

Impact Factor: 2.59 · DOI: 10.1021/ie3030467

3 AUTHORS:

François Grégoire
Laval University
2 PUBLICATIONS **1** CITATION
SEE PROFILE

Louis Gosselin
Laval University
90 PUBLICATIONS **1,078** CITATIONS
SEE PROFILE

Houshang Alamdari
Laval University
92 PUBLICATIONS **1,013** CITATIONS
SEE PROFILE

I&EC research
Industrial & Engineering Chemistry Research

Article

pubs.acs.org/IECR

Sensitivity of Carbon Anode Baking Model Outputs to Kinetic Parameters Describing Pitch Pyrolysis

François Grégoire,[†] Louis Gosselin,*[,†] and Houshang Alamdari[‡]

[†]Département de génie mécanique, Université Laval, Québec City, Québec, Canada, G1V 0A6

[‡]Département de génie des mines, de la métallurgie et des matériaux, Université Laval, Québec City, Québec, Canada, G1V 0A6

ABSTRACT: Carbon anode blocks, used in aluminum electrolysis cells, are usually baked in furnaces for several days, during which they release volatiles due to pitch pyrolysis. Therefore, numerical modeling of anode baking furnaces has to include some representation of pitch pyrolysis via a set of kinetic parameters. These kinetic parameters can vary with raw materials and baking parameters and are tedious to determine experimentally. In this work, we studied how the main outputs of an anode baking model are affected by the variance of the kinetic parameters. Results show that certain model outputs are not considerably influenced by changes in the kinetic parameters (e.g., spatial variation of anode porosity, maximum heating value from volatiles), while others are significantly affected (e.g., time evolution of anode porosity, time of maximum heating value of volatiles, internal pressure of anode), in particular by activation energy variability.

1. INTRODUCTION

According to the International Aluminum Institute, the world aluminum industry produced approximately 41 million tons of new (primary) aluminum in 2010. Nowadays, the largely dominant technology used to produce aluminum is the Hall-Héroult process, using prebaked carbon anodes. Anodes are literally consumed during this process (roughly speaking, the carbon of the anodes combines with the oxygen of the alumina (Al_2O_3) to form CO_2, thus leaving "pure" aluminum to be tapped out).[1] As a consequence, aluminum smelters need to continuously produce large quantities of anodes to replace those that have been consumed in electrolytic cells. The lifetime of an anode in a cell is approximately 22−30 days.[1] The main steps followed for the production of an anode are: mixing of raw materials (i.e., ∼65% petroleum coke, 15% binder pitch, and 20% recycled anode butts), vibro-compaction, and baking for approximately 2 weeks, followed by anode roding.

One of the problems that plagues the industry is the great variability of the properties of anodes, namely, thermal shock resistance, electrical resistivity, air/CO_2 reactivity, and density. The anode variability causes various difficulties in potroom operation and control and translates into financial losses and environmental drawbacks. This variability originates from the raw materials, anode formulation, anode forming, and anode baking. For example, during their baking, anodes experience different temperature histories depending on where they are positioned in the baking furnace, which results in different final properties. Furthermore, on the basis of the current market, raw materials from different suppliers do not exhibit a constant composition (e.g., petroleum coke can contain 1−4 wt % of sulfur depending on supplier).[2] This is particularly true nowadays; with the rising price of raw materials, nontraditional materials are increasingly used.

As a consequence, when it comes to managing, controlling, or simply modeling the anode production line, it is usually difficult to obtain precise or sure values for the properties of materials or adequate constitutive laws. Obtaining these properties can be tedious, time-consuming, and costly. Therefore, an important question that arises is: to what extent a given input property with variability might affect the outcomes of a given process?

In this paper, we investigated the sensitivity of an anode baking model to the kinetic parameters that characterize the release of volatiles during baking. The objectives of the present paper are to: (i) quantify how the variance of the main outputs of interest is affected by the variance of the kinetic parameters and (ii) provide guidance regarding the necessity to perform new kinetic parameters measurements.

Schematic views of a typical anode baking furnace (ABF) is shown in Figures 1 and 2. Anodes are stacked between porous refractory walls separated by a flue channel in which hot gases flow. Green anodes are loaded at the inlet of the furnace, and blowing ramps supply ambient air in the flue channels at the other side. The anodes will first be preheated for ∼3−5 days. During the preheating, they will release volatiles (H_2, CH_4, tar)

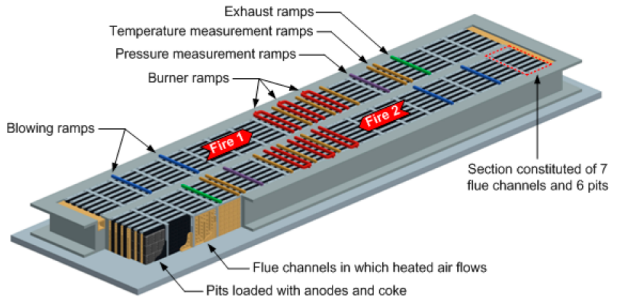

Figure 1. Schematic representation of an anode baking furnace.

Received: November 6, 2012
Revised: January 18, 2013
Accepted: February 20, 2013
Published: February 20, 2013

dx.doi.org/10.1021/ie3030467 | *Ind. Eng. Chem. Res.* 2013, 52, 4465−4474

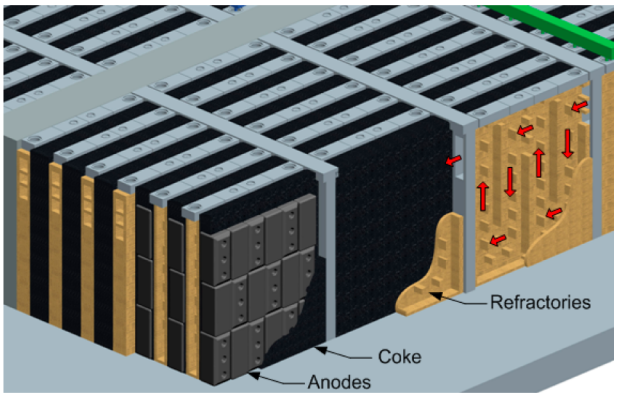

Figure 2. Schematic representation of the pit and the flue wall.

that will burn in the flue. The combustion of volatiles accounts for approximately 40−50% of the required heating, the rest being provided by natural gas; see burner ramps on Figure 1. Finally, cooling of the anodes will preheat incoming air from blowing ramps.

Mathematical models of ABFs have been published starting in the 1980s. Their application and complexity vary, but they can be separated into 3 categories. The majority of these models require some kind of kinetic parameters to account for the pyrolysis of volatiles during baking.

The first category is "solids models" including only the anode, coke, and refractories.[3−7] Essentially, the transient heat conduction equation is solved in order to obtain the temperature history of the solids during baking. This is the only type of model that does not use kinetic parameters nor pyrolysis equations. The release of volatiles and the heat provided by their combustion are hidden in the Dirichlet or Neumann boundary conditions applied at the surface of the refractories.

The second category is "overall models" where the ABF is treated as a counterflow heat exchanger: the gas is flowing from inlet to outlet and the solids are "moving" in the opposite direction at a speed corresponding to a section length divided by the fire time (roughly 5 m per day).[8−18] The core of these models is 1D momentum and energy balances along the furnace accompanied by the conduction equation (1D or 2D) for the temperature of solids. The only boundary conditions needed are the flow conditions and temperature of solids at the inlet (or outlet) of the baking cycle. Pyrolysis equations with kinetic parameters are used for the calculation of a corresponding heat source in the energy balance of the flue gas along the furnace. These models provide the whole "portrait" of a baking cycle, which is why they are considered as predictive models: on the basis of few inputs, they give a lot of information on the furnace operation.

The third category is "locally detailed models" which include all (or most) of the multiple phenomena that take place in the ABF: heat transfer (conduction, convection, radiation), pyrolysis kinetics, species mass transport, turbulent gas flow, and combustion of natural gas/volatiles.[19−24] Those models can require significant CPU time in 2D or 3D. They are useful in order to optimize a precise aspect of the furnace (e.g., flue geometry) but are limited for the evaluation of the overall furnace operation. The present work is largely inspired by these models.

2. KINETIC PARAMETERS TO DESCRIBE PITCH PYROLYSIS

Typical anodes contain 13−18 wt % of coal tar pitch that acts as a binder between the coke particles. Pitch has a very complex chemical composition of thousands of molecules (~10 000) dominated by polycyclic aromatic hydrocarbons (PAH).[25−27] During the baking process, a fraction of the pitch will be volatilized by a number of phenomena: distillation, cracking, and polymerization.[28−30] All these phenomena are comprised here under the term "pyrolysis". The remaining part of the pitch will be carbonized to coke. Because the number of volatile compounds and chemical reactions is too large to be all characterized and modeled, it is common practice to consider simplified kinetics for the pitch pyrolysis of anodes of the aluminum industry.[31,32] The simplified kinetics assumes irreversible parallel reactions where the pitch is volatilized in 2 categories of gases: condensables (all PAH grouped under the label "tar") and noncondensables (H_2 and CH_4).[31,32]

In a detailed model of anode baking, it is convenient to represent the local rate of density change for solid species "i" as:[23]

$$\frac{\partial \rho_{s,i}}{\partial t} = -\rho_{s,i0} A_i \exp\left(-\frac{E_i}{RT}\right)\left(\frac{\rho_{s,i}}{\rho_{s,i0}}\right)^{n_i} \quad (1)$$

This approach relies on three kinetic parameters (A_i, E_i, and n_i) for each species "i" of the model (i.e., i = H_2, CH_4, tar).

Many studies on pitch pyrolysis have been performed in the past. A list of the major contributions in this field can be found in ref 32, in addition to a comparative study of various pitches in ref 33 and more recent studies in refs 34 and 35. However, most results are not straightforwardly applicable to the anodes of the aluminum industry for various reasons: the size of the samples is very small compared to that of the anodes, the pitch is considered alone (i.e., not mixed with coke), the heating rate and temperature range are not representative of the anode baking process, and the three pyrolysis species (H_2, CH_4, and tar) are sometimes grouped under an overall kinetic representation (e.g., one set of A, E, and n for representing all pyrolysis phenomena). The methods for the determination of kinetic parameters A, E, and n from thermogravimetric data are also numerous. They can be classified into 3 categories: differential, integral, and special methods. An extensive comparison of these methods is available in ref 36. The work of Tremblay and Charette[32] is the major source of experimental results for pyrolysis of the carbon anodes of the aluminum industry. They modeled the pyrolysis by 3 single-step parallel reactions of n^{th} order for H_2, CH_4, and tar. It is worth to point out that this representation does not aim at describing the highly complex scheme of elementary reactions taking place during pitch pyrolysis. The results aim at quantifying the rate of volatilization of the major species for modeling purposes. They used a classical differential method (see eq 19 in ref 36) to determine A_i, E_i, and n_i. According to their work, the orders of reaction are 1.1, 0.8, and 0.7, respectively, for H_2, CH_4, and tar. The activation energy is found to vary with the heating rate (a, expressed here in K/h) with the following form for the three species i:

$$E_i = C_{1,i} \ln(a) + C_{2,i} \quad (2)$$

Furthermore, the typical form of the compensation effect[37] was retained in order to correlate A with E:

dx.doi.org/10.1021/ie3030467 | Ind. Eng. Chem. Res. 2013, 52, 4465−4474

$$\ln A_i = C_{3,i}E_i + C_{4,i} \quad (3)$$

All constants $C_{1,i}$ to $C_{4,i}$ have been deduced from measurements (12 constants) and are reported in Table 1. The same values

Table 1. Value of the Constants for Correlations (2) and (3), Taken from Ref 32

	H_2	CH_4	tar
C_1	5.882	10	4.167
C_2	57.65	76	35
C_3	0.233	0.225	0.273
C_4	−10.39	−11.325	−6.417

have been used in the present work for the calculation of A and E. These constants represent averaged values obtained with a few samples (∼10) at 4 different heating rates between 5.2 and 42.7 K/h.

As can be seen from eq 3, there is a relationship between the activation energy and the pre-exponential factor. However, this relation is not to be considered "exact" in any case.[37] Eqs 2 and 3 do not represent detailed chemical processes, and thus variations are likely to occur around the values obtained with these equations in practice. The variability of A is approached here by assuming that, for a given value of E, the value of A can vary around the mean value provided by eq 3. Therefore, in the present study, the values of E and A are free to vary randomly within a certain distribution around their corresponding means calculated with eqs 2 and 3 (see Section 3.3). The correlation corresponding to eq 3 is thus preserved on average, and at the same time, E and A can vary independently around the average values of eqs 2 and 3 (see Section 3.3).

3. DISCUSSION ON VARIANCE OF KINETIC PARAMETERS OF CARBON ANODES

Although correlations such as eqs 2 and 3 are quite useful, the question of the uncertainties or variability of the kinetic parameters of baking anodes has not been studied extensively. Variations associated with the values of the kinetic parameters come from several sources: precision of measurements (e.g., temperature, mass, concentration, heating rate), uniformity in temperature within the sample during testing, assumptions in the postprocessing of the measurements (i.e., representation with only three species, tar is assumed to pyrolyze only between 150 and 550 °C, etc.), and the mathematical treatment of the data (e.g., integral, differential, and special methods do not necessarily give the same values of kinetic parameters from the same set of data).[38] Finally, different types of coke and pitch can be used, having different kinetic parameters. Therefore, it should be clear that there might be a significant variance of the kinetic parameters and that their values can hardly be known exactly. When they are "input" in baking furnace models for quantifying the volatilized gases (that will bring roughly 40−50% of the energy required for baking), one should expect to observe a variance in the outputs of the model due to variations of kinetic parameters. Although it is difficult to estimate precisely the variance of the kinetic parameters, we will try in the following subsections to at least estimate their orders of magnitude.

3.1. Differences between Test Samples in Ref 39. Ref 39 is the master's thesis behind ref 32. It provides detailed results achieved by repeated testing under the same conditions (repeatability). For example, at a rate of heating of 21.4 K/h, 4 tests were performed with a 220 g sample and 2 tests with a 55 g sample. Calculating the standard deviation for this distribution of points, we obtain $\sigma_{E,i}/E_i$ of ∼3%, 11%, and 3% for i = tar, H_2, and CH_4, respectively. Similarly, for $\sigma_{\ln A,i}/\ln A_i$, we obtain 4%, 14%, and 4% for i = tar, H_2, and CH_4, respectively. Note that considering only the larger samples reduces the standard deviation, but the ratios $\sigma_{E,i}/E_i$ and $\sigma_{\ln A,i}/\ln A_i$ all stay between 2% and 4%. Although the number of data points is very small, this shows that there is a nonzero variability even when the same pitch and coke are used. This might be seen as a lower bound value for the variability of the kinetic parameters, i.e., it is unlikely to observe a variability below ∼2−4% between repeated measurements.

3.2. Variations Induced by Raw Materials. Another motivation of the present work is that unconventional anode materials are increasingly used in today's aluminum industry. As the sweet crude oil resources are declining and the prices are rising, the trend in the petroleum refining industry is to process more sour crude feed stocks. This results in an increase of sulfur and metal impurities in the petroleum coke.[40,41] It is difficult to determine whether these impurities have a significant effect on the kinetics of pitch pyrolysis (it is beyond the scope of this paper), but chances are that they do: Maroto-Valer et al.[42] showed that sulfur additions promote the polymerization of coal tar pitch and therefore modify the kinetics.

Another source of kinetic parameter variation can be attributed to the origin of the coal tar pitch and the content of inorganic contamination. The variation of kinetic parameters due to that factor is hard to quantify. Charette et al.[33] compared 10 different pitches used in carbon electrodes for steel industry. Each pitch having different properties but no information was given regarding the contaminant content. Although they came to the conclusion that the overall performance of every pitch was similar, there is a large variation of the kinetic parameters between different pitches in Table 3 of ref 33. For example, making a similar analysis as in Section 3.1, we obtain σ_E/E and $\sigma_{\ln A}/\ln A$ of 27% and 33%, respectively, for the condensable volatiles at temperatures between 350 and 500 °C.

Finally, Bouchard[43] observed a catalytic effect of the petroleum coke on the PAH release when coal tar pitch is mixed with coke. Significant variations of the volatile release behavior were found, depending on the mixture considered and on the heating rate.

3.3. Representation of Uncertainties in This Paper and Choice of Random Variables. We will assume that, at a given heating rate, the activation energy can be described by a normal distribution with standard deviation $\sigma_{E,i}$:

$$E_i = N(\bar{E}_i, \sigma_{E,i}) \quad (4)$$

As for the pre-exponential factor, it will be represented by

$$\ln A_i = N((C_{3,i}E_i - C_{4,i}), \sigma_{A,i}) \quad (5)$$

At this point, we considered the order of reaction as being "certain". This means that, with three species, 6 random variables are required to describe the problem. We call them: $X_{E,i}$ and $X_{A,i}$ with i = tar, H_2, and CH_4. These variables can take values between 0 and 1 with equal probability. The mapping between the X's and the physical parameters (x) is thus:

$$x = \mu + \sigma\sqrt{2}\,\mathrm{erf}^{-1}(2X - 1) \quad (6)$$

dx.doi.org/10.1021/ie3030467 | Ind. Eng. Chem. Res. 2013, 52, 4465−4474

Considering the discussion in previous subsections, the value of $\sigma_{E,i}$ and $\sigma_{A,i}$ has been fixed to 15% in the present study.

4. NUMERICAL MODEL OF ANODE BAKING

To study the sensitivity of anode baking to the kinetic parameters, we consider a 1D model that includes the porous anode, the packing coke, and the flue wall, as shown in Figure 3. The model was inspired by the work reported in ref 21, and due to space limitation, it is only summarized here.

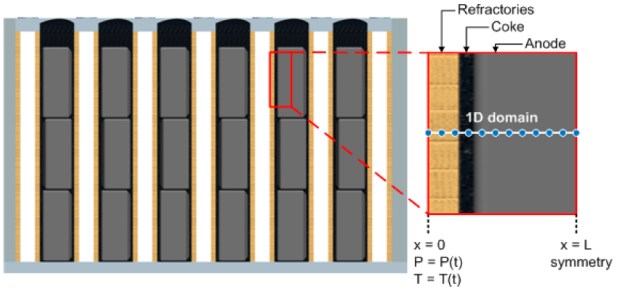

Figure 3. Schematic representation of the 1D domain considered in the model.

In the anode, the total solid density is made out of four components:

$$\rho_{s,tot} = \rho_{s,coke} + \sum_{i=1}^{3} \rho_{s,i} \tag{7}$$

with i = H_2, CH_4, and tar. Strictly speaking, tar is a mixture of different molecules and only an average molecule is considered here. The solid densities are volume-averaged, i.e., mass of solid per unit of total volume. The first density on the right-hand side of eq 7 is constant; i.e., it does not vary in time since coke does not pyrolyze. However, the three terms of the summation vary in time because of pyrolysis that converts solids into gases. The rate of density change for solid species "i" is as in eq 1. The porosity and permeability of the anode adapts to the release of solids into gases.

The numerical model solves 4 gas species conservation equations (tar, CH_4, H_2, and air) and includes a source term for the generation of volatiles based on eq 1. Multicomponent diffusion was accounted for through the use of Wilke's approach,[44] which consists of calculating an effective diffusion coefficient for each species. Pressure is found on the basis of the ideal gas law, and Darcy's law is used to determine gas velocity distribution.[45] The permeability of the anode varies linearly between an initial (K_G) and a final value (K_B) as:

$$K = K_G\alpha + (1 - \alpha)K_b \tag{8}$$

where α is a pyrolysis progress variable which is 1 initially and 0 when the conversion of solids into gases is completed:

$$\alpha = \frac{\sum_i \rho_{s,i}}{\sum_i \rho_{s,i0}} \tag{9}$$

.This approach is often used in the modeling of thermo-physical properties of pyrolyzing biomass.[46,47]

The energy equation determines the temperature distribution by assuming local thermal equilibrium and neglecting the energy required for pyrolysis. On the basis of literature, this heat of reaction is assumed to be small,[30] and its effect is lumped in the effective heat capacity of the anode,[19] which is a function of local temperature taken from ref 48. To our knowledge, only qualitative information regarding the endothermicity or exothermicity of the reactions is available in the literature,[30,43,49] and the heat of reaction has never been included in the energy equation for the anodes in a baking furnace model.

The following boundary conditions were used (see Figure 3). At $x = 0$, the pressure is imposed (it is the pressure in the flue channel). We also assumed that the temperature evolution $T(t)$ is known at that position; i.e., the flue channel was not modeled in the present work. At $x = L$, symmetry is assumed. The initial conditions are: solids at ambient temperature and pressure (298.15 K and 1 atm, respectively). The simulation was for the heating sections of an ABF, i.e., for time up to 144 h.

The model was implemented in a commercial finite element software.[50] In the end, the model provides velocity, pressure, temperature, and concentrations as a function of time and position. Properties were taken from literature,[21,48,51] and most of them vary with temperature and porosity based on empirical correlations developed from measurements.

Our model was validated by producing results similar to those published in ref 21. It was not possible to reproduce the exact same results because some physical and thermal properties were not given in the article. Nevertheless, our results were close to theirs and exhibited the same trends as Figures 5−13 of ref 21. For example, we obtained similar anode temperature with a difference always smaller than 9%, and very similar maximum concentrations of H_2 and CH_4 in the solids (less than 14% and 9% difference, respectively). The largest differences were observed for the maximum tar concentration (58%) and maximum overpressure (33%), but this is due to (i) different thermal properties which have shortened the duration of tar pyrolysis by about 15 h and (ii) the last species to pyrolyze (H_2) has maximum release rate and concentration occurring at a slightly different temperature, but this difference in temperature results in a significant difference in the pressure calculated by the ideal gas law ($p = c_{tot}RT$). Figure 17 of ref 21 presented results with diffusion included, and once again, we obtained similar curves. Therefore, the model was considered to yield satisfactory results. Note that a mesh of 101 quadratic Lagrangian elements was used, since a finer mesh did not change the solution. The time step was allowed to vary according to variable-order variable-step-size backward differentiation formulas.[50] The solver was set to stop if time step went inferior to 0.1 s, indicating difficulty to converge.

5. MODEL OUTPUTS OF INTEREST

A typical example of results obtained from the numerical model is shown in Figure 4. The results are functions of time and position. To facilitate the analysis, we carefully selected a certain number of scalar outputs of interest that are intimately related to pitch pyrolysis. These scalars will be described below.

In Figure 4c, one can observe how pressure varies at various points in anode. As the volatiles are released and temperature increases, pressure builds up. Eventually, pressure starts to go down as pyrolysis is finished (i.e., all solid that could pyrolyze has actually been pyrolyzed). Two pressure-related outputs will be considered here. The first one is the maximal pressure achieved in the domain. We expressed it in a dimensionless form:

dx.doi.org/10.1021/ie3030467 | Ind. Eng. Chem. Res. 2013, 52, 4465−4474

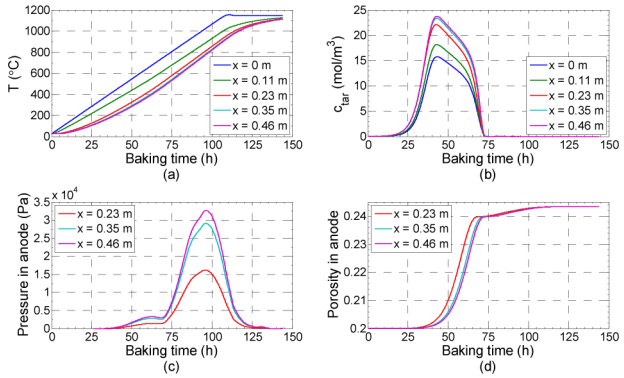

Figure 4. Typical results achieved from the numerical model ((a) temperature at various points in solids, (b) gaseous tar concentration at various points in solids, (c) internal gauge pressure at various points in anode, and (d) evolution of porosity at various points in anode).

$$Y_{P,1} = \frac{P_{max} - P_{atm}}{P_{atm}} \tag{10}$$

Maximal internal pressure is an important quantity: too large internal pressure can result in cracks in the anodes, which is detrimental to the mechanical and electrical properties of the anodes.[52] Therefore, it is important to verify whether changes of kinetic parameters affect internal pressure. The second pressure-related output parameter chosen is the time at which the peak pressure occurs:

$$Y_{P,2} = \frac{t(P = P_{max})}{\tau} \tag{11}$$

where τ is the total time simulated (144 h in the present study).

Volatiles evolved during pitch pyrolysis have a critical role in the baking curve of the anodes since they will burn in the flue and provide baking energy. The quantity of volatiles and the time at which the pyrolysis takes place have a major influence on the anode quality and the natural gas consumption of the furnace. We defined two outputs in order to quantify the heating value of the volatile flux coming out at the surface of the refractories: the first one is the maximum heating value occurring during the simulation

$$Y_{HV,1} = \frac{[\dot{m}_{H_2}\chi_{H_2} + \dot{m}_{CH_4}\chi_{CH_4} + \dot{m}_{tar}\chi_{tar}]_{max}}{(\rho_{H_2,0}\chi_{H_2} + \rho_{CH_4,0}\chi_{CH_4} + \rho_{tar,0}\chi_{tar})L_{anode}/\tau} \tag{12}$$

where $\dot{m}_i$ is the mass flux (kg m^{-2} s^{-1}) of species i at the refractory surface and χ_i is the heating value (MJ/kg). For the sake of this paper, we selected the following heating values for H_2, CH_4, and tar, respectively: 120, 50, and 35 MJ/kg.[53] The denominator in eq 12 represents the heating value contained initially in the pitch of the anode. The second output is the time at which the maximum heating value occurs:

$$Y_{HV,2} = \frac{t(Y_{HV,1})}{\tau} \tag{13}$$

Next, we defined two porosity-related outputs which are intimately related to anode density and thus to pitch pyrolysis. The first output is the time at which the average porosity of the anode is halfway between its initial and final value

$$Y_{\varepsilon,1} = \frac{t(\bar{\varepsilon} = \varepsilon_i + \Delta\varepsilon/2)}{\tau} \tag{14}$$

The second porosity output is the maximum difference of porosity between anode surface and anode center that occurs during the baking

$$Y_{\varepsilon,2} = \frac{[\varepsilon(x_1) - \varepsilon(x_2)]_{max}}{\varepsilon_i} \tag{15}$$

The porosity directly affects the gas permeability and thus the volatiles transport dynamics. An important variation of $Y_{\varepsilon,1}$ and $Y_{\varepsilon,2}$ would indicate that the volatiles evacuation process can be accelerated or slowed by variations of the pitch kinetics.

Other parameters were also considered (e.g., temperature difference between anode surface and anode center, maximum heat flux toward solids), but their variations were very small. Moreover, the fact that we impose a constant heating rate at the surface of refractories makes those parameters less appealing since they are regulated to a large extent by this boundary condition.

6. SAMPLING STRATEGY AND SENSITIVITY ANALYSIS

Since the model is relatively quick to solve (less than 30 s per simulation), we decided to use a Monte Carlo approach. Many sets of the six variables $X_{E,i}$ and $X_{A,i}$ (with i = tar, H_2, and CH_4) were generated randomly. Each random variable was translated into the original input variables with the mapping described previously (e.g., $X_{E,tar} \rightarrow E_{tar}$). All sets of input variables were used to perform a distinct simulation. Then, the output variables described in Section 5 were determined on the basis of the simulation results. A total of 17 600 simulations were performed in this way. This database was then exploited to determine the sensitivity of each output to variations of the inputs with three approaches that are outlined in the following subsections.

6.1. Coefficients of Variation. At first, the coefficient of variation (CV) of each output was calculated. This percentage expresses the standard deviation of the output as a percentage of the mean:

$$CV_Y = \frac{\sigma_Y}{\mu_Y} \times 100 \tag{16}$$

Large CV_Y values mean that there is a large dispersion of the Y-values obtained from the model when the kinetic parameters were varied.

Results are reported in Figure 5. For all the Y's, CV_Y did not exceed 17%. That is to say, no output was outrageously affected by the variation of the inputs. The largest CV, 16.7%, was for $Y_{\varepsilon,1}$ and $Y_{HV,2}$. A large CV for $Y_{\varepsilon,1}$ (time at which half of the pitch has pyrolyzed) is not a surprise since the porosity is directly related with the variation of density of the anode:

$$\varepsilon = 1 - \frac{\rho_{bulk}}{\rho_{real}} \tag{17}$$

and the bulk density is directly related to pyrolysis parameters. A large CV for $Y_{HV,2}$ is interesting since it means that the maximum "heating value flux" of volatiles in the flue can happen at quite different times during the baking and could possibly modify or shift the baking curve ($T_{anode}(t)$). In the present model, the maximum flux occurred at an average time of 59 h, and a CV of 16.7% means that this moment can be shifted by ±4 h.

The pressure-related outputs $Y_{P,1}$, and $Y_{P,2}$ had CV's of 9.1% and 11.9%, respectively. As mentioned earlier, they represent the maximum pressure in the anode and the time at which it

dx.doi.org/10.1021/ie3030467 | Ind. Eng. Chem. Res. 2013, 52, 4465−4474

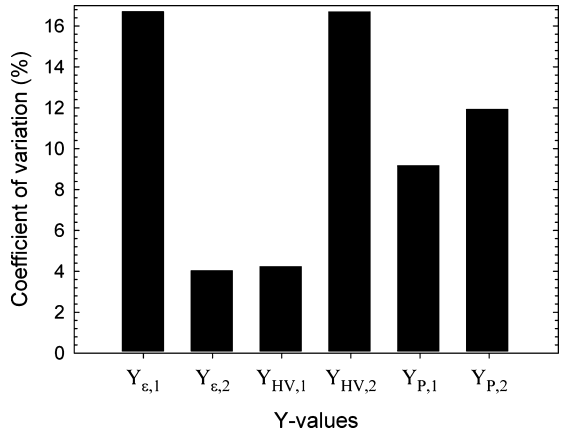

Figure 5. Coefficients of variation obtained for various outputs of baking model.

occurs. If the kinetic parameters of the 3 species are such that the pyrolysis is "compressed" in a shorter time, the maximum pressure will assuredly rise. It is hard to quantify critical overpressure since, to our knowledge, there is no source of experimental results for comparison. Moreover, the model is 1D and supposes gas flow in one direction only. Therefore, the pressure calculated may not be precise, but it provides an indication that variable raw materials have the potential to rise (or lower) the internal overpressure. The CV of 11.9% for $Y_{P,2}$ means that the maximum pressure can happen at ±7 h around the average time of 93 h in this model. It is reasonable to say that the anodes have a heating rate of about 9 °C/h at this time of the baking; therefore, a shift of ±7 h represents a difference of ±60 °C in the anodes when the maximum pressure occurs. Therefore, the maximum pressure can be significantly higher or lower depending on whether it occurs sooner or later according to ideal gas law.

Finally, the output parameters $Y_{\varepsilon,2}$ and $Y_{HV,1}$ showed little variations both with a CV of about 4%. In other words, the spatial variations of density in the baked anodes and the peak value of the heating potential flux are not affected by changes in the kinetic parameters. Consequently, those parameters are not considered for the rest of this study as they are weakly influenced by variations of the input kinetic parameters.

6.2. Linear Regression. Although the approach outlined in Section 6.1 allowed one to determine which outputs were most affected by the inputs variability, the coefficient of variation provides no information on which inputs are the most influential. Therefore, a second approach was considered, which consisted of linear regression with the following form

$$Y_n^* = b_0 + \sum_{i=1}^{6} b_{X_i} X_{i,n} \tag{18}$$

where n goes from 1 to 17 600, the number of model runs. Regression coefficients b_0 to b_6 are determined by minimizing the quadratic error between the actual values of Y and the ones obtained by the regression, i.e., by minimizing

$$E = \sum_{n=1}^{17600} (Y_n - Y_n^*)^2 \tag{19}$$

Instead of using directly the raw regression coefficients (the b's), a more robust approach[54] is to calculate the standardized regression coefficients (SRC)

$$\beta_{X_i} = b_{X_i} \frac{\sigma_{X_i}}{\sigma_Y} \tag{20}$$

In short, the SRCs express the standard deviation change in Y when X_i is changed by one standard deviation, holding all other X_i constant. They offer a measure of the effect of an input X_i that is averaged over a set of N possible values of the other factors. By computing the sum of the squares of the SRC, $\sum_i (\beta_{X_i})^2$, we obtain a number representing the fraction of linearity of the model.[54] In our study, if this sum was superior to 0.8 for a given output, we considered that the linear model successfully explains which of the 6 inputs were the most influential. Below 0.8, we considered that the nonlinearity was too large for the approach of this section to yield satisfactory results, thus another approach was considered (see Section 6.3).

The linear regression was successful (i.e., $\sum_i (\beta_{X_i})^2$ was larger than 0.8) for 3 outputs. The results are reported in Table 2 and shown in Figure 6. At first, we observe that the activation

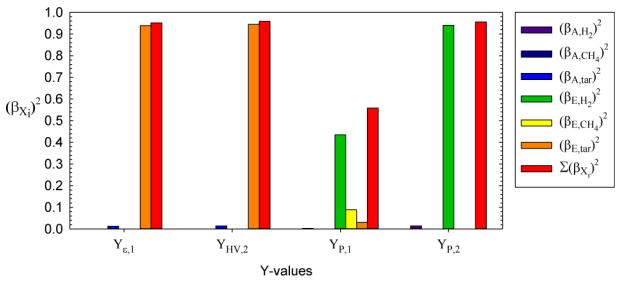

Figure 6. Standardized regression coefficients of Y-values.

energy has much more influence than the pre-exponential factor. The activation energy of the tar was clearly the determinant factor in the variation of $Y_{\varepsilon,1}$ and $Y_{HV,2}$. Since solid tar has the largest mass fraction (~90%) in the fraction of coal tar pitch that will pyrolyze, this is the species that mostly affects the change in porosity. The influence of the tar on $Y_{HV,2}$ has the same explanation: despite the fact that the tar heating value is lower than that of H_2 and CH_4, the larger mass of gaseous tar dictates the variation of the time at which the maximum heating value occurs. Since the tar is the first volatile species to be released, the shift of the release curve can have a significant effect on the control of the pitch burn in the furnace.

Table 2. Results of the Linear Regression

	$(\beta_{A,H_2})^2$	$(\beta_{A,CH_4})^2$	$(\beta_{A,tar})^2$	$(\beta_{E,H_2})^2$	$(\beta_{E,CH_4})^2$	$(\beta_{E,tar})^2$	$\sum(\beta_{X_i})^2$
$Y_{\varepsilon,1}$	5.2×10^{-06}	2.6×10^{-08}	1.3×10^{-02}	1.9×10^{-05}	1.9×10^{-04}	9.4×10^{-01}	0.95
$Y_{HV,2}$	1.8×10^{-07}	2.1×10^{-07}	1.4×10^{-02}	1.6×10^{-04}	5.8×10^{-05}	9.4×10^{-01}	0.96
$Y_{P,1}$	2.8×10^{-03}	7.4×10^{-04}	3.7×10^{-04}	4.3×10^{-01}	8.9×10^{-02}	3.1×10^{-02}	0.56
$Y_{P,2}$	1.4×10^{-02}	2.4×10^{-06}	5.3×10^{-06}	9.4×10^{-01}	8.5×10^{-05}	1.2×10^{-03}	0.96

dx.doi.org/10.1021/ie3030467 | Ind. Eng. Chem. Res. 2013, 52, 4465−4474

The process control system of a baking furnace has to be carefully adjusted with the peak of volatiles in order to provide adequate ignition temperature and sufficient oxygen for the combustion of nearly 100% of the volatiles.[55] This is especially critical for the early volatiles released because the flue temperature may not be high enough for the volatiles to reach their ignition temperature before they reach the exhaust ramp.[54] Moreover, the oxygen content is low (less than 10%) in this section of the furnace,[52,53] which can also lead to incomplete combustion of volatiles. This results in wasted energy and higher natural gas (or fuel) consumption and soot deposits in the exhaust system and the gas treatment plant. Those deposits generate high maintenance costs and can even lead to fire incidents in ducts where cleaning is not possible.

Regarding $Y_{P,2}$, the variation of the time at which maximum overpressure in the anode occurs is attributed to the fluctuation of H_2 activation energy. This maximum pressure occurred at about 93 h of baking on average, when the anode is at an average temperature of 770 °C and the release of H_2 is at its maximum.

For the output $Y_{P,1}$, the fraction of linearity was relatively small (0.56, see Table 2). Although variations in the activation energy of H_2 seemed to be the most influential factor, nonlinearity, i.e., interactions between inputs, proved to be important.

6.3. Variance-Based Method. Since nonlinearity was important for $Y_{P,1}$, a third approach was also considered. This third approach was to use a variance-based method which relies on the decomposition of the variance in the model output. Various variance decomposition techniques are available,[54] each having their particularities regarding the sampling scheme and the number of required model runs. We chose a Fourier-based technique described in ref 56, because this method has the advantage that existing data from previous model runs can be used directly at no extra cost. We exploited our set of simulations in order to compute the first-order and second-order indices for $Y_{P,1}$. The first-order indices (S_i) are a measure of the contribution of input X_i to the variance of output Y. It represents the average fraction of variance of output Y that could be eliminated if input X_i could be fixed. Second-order indices (S_{ij}) measure interaction effects between any combinations of 2 inputs X_i and X_j with $i \neq j$. Similarly to the first-order indices, they represent the average fraction of variance of output Y that could be eliminated if 2 inputs X_i and X_j could be fixed, minus their first-order effects. When a set of N input parameters X_i are independent, the total variance of an output Y can be decomposed as

$$V(Y) = \sum_i V_i + \sum_i \sum_{j>i} V_{ij} + \sum_i \sum_{j>i} \sum_{k>j} V_{ijk} + \ldots + V_{12\ldots N} \quad (21)$$

where V_i is the variation of the expected value of Y for every value of X_i:

$$V_i = V(E(Y|X_i)) \quad (22)$$

V_{ij} is similar but the variance due to first-order effects has to be subtracted:

$$V_{ij} = V(E(Y|X_i, X_j)) - V_i - V_j \quad (23)$$

Dividing both sides of (21) by $V(Y)$:

$$1 = \sum_i S_i + \sum_i \sum_{j>i} S_{ij} + \sum_i \sum_{j>i} \sum_{k>j} S_{ijk} + \ldots + S_{12\ldots N} \quad (24)$$

For linear models, the first-order indices are equal to the squared standardized regression coefficients ($S_{X_i} = (\beta_{X_i})^2$).[54] Therefore, we expect that the outputs for which linear regression was successful ($Y_{\varepsilon,1}$, $Y_{HV,2}$, and $Y_{P,2}$) have first-order indices similar to their respective SRCs. The results for first-order indices are shown in Figure 7. For linear outputs, we

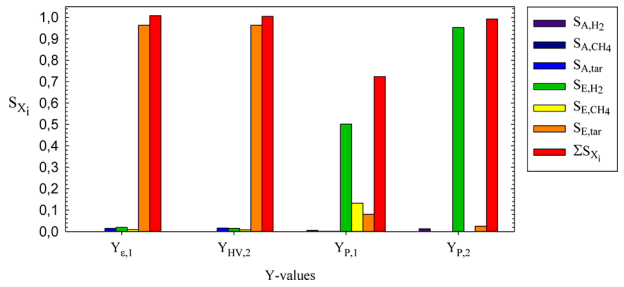

Figure 7. First-order sensitivity indices of Y-values.

see that the major first-order indices are very similar to their corresponding SRCs; the difference is within 3%. For example, $(\beta_{E,\,tar})^2 = 0.94$ and $S_{E,tar} = 0.96$. For the other indices that have low values (<0.1), their value can be very different than their corresponding SRC, but this has no effect on the quality of the analysis since they simply represent non important parameters. For $Y_{P,1}$ (maximal pressure), i.e., the parameter for which the variance was not well captured by the linear regression, the sum of first-order indices explains 72% of the total variance whereas the sum of squared SRCs explained 56% of the linearity. Therefore, we gain some insight on which input parameters affect the variance. We get the same relative importance of inputs X_i: it is the activation energy of H_2 that is mainly responsible for the main effects, followed by those of CH_4 and tar.

In order to fully explain the variance of $Y_{P,1}$, we now look at the second-order indices obtained with the Fourier-based technique of ref 56. Figure 8 shows a bar graph with the second-order indices obtained. There is clearly an interaction

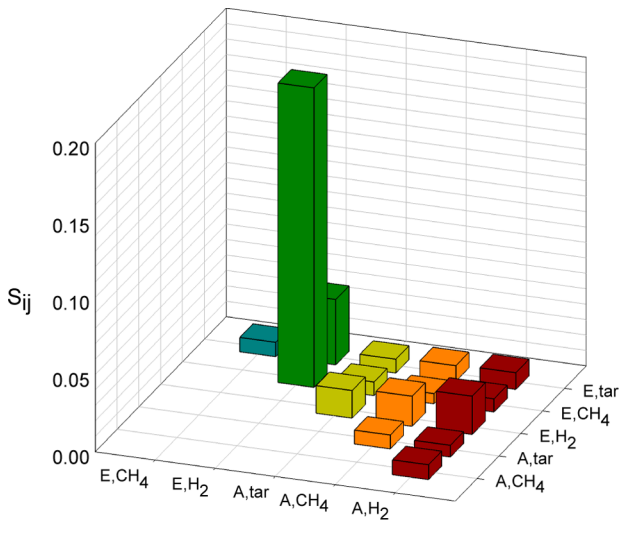

Figure 8. Second-order sensitivity indices for output $Y_{P,1}$.

dx.doi.org/10.1021/ie3030467 | Ind. Eng. Chem. Res. 2013, 52, 4465−4474

effect between activation energies of H_2 and CH_4. Since the pyrolysis of those species typically occurs at temperatures over 550 °C,[32] they can produce high internal pressure according to ideal gas law if their releases overlap. The variance of output $Y_{P,1}$ is now fully explained: the sum of the S_i plus the interaction effect $S_{E,H2\text{-}E,CH4}$ is approximately equal to 1. According to eq 24, the first and second-order indices are sufficient to explain the total variance of $Y_{P,1}$ since they sum to 1. Therefore, there was no need to proceed to calculating higher order indices.

7. DISCUSSIONS

On the basis of the sensitivity analysis, we can pinpoint critical parameters that have significant effects on the outputs of baking models described in Section 4 and, ultimately, on the outputs of actual baking furnaces. The analysis clearly showed that the activation energies are the most influential parameters for the outputs of interest, and they should be accurately determined experimentally if one is going to use this model. Even if a more complex kinetic model is used, chances are that the activation energies remain the most influential parameters.

In view of our results, one can make the following statements:

- The peak value of the heating potential flux as well as the spatial variations of porosity during baking are not affected significantly by changes of the kinetic parameters.
- The activation energy of tar should be well determined in order to predict the evolution of porosity during baking. The porosity affects the gas permeability of the anode and, consequently, the transport dynamics of the volatiles toward the flue channel.
- The activation energy of tar should be well determined in order to predict the time at which the maximum heating value from volatiles occurs in the flue channel. A good prediction of when volatiles are released is very important in a complete baking model (including the flue channel) since they contribute to 40−50% of the baking energy.
- The activation energy of H_2 and CH_4 should be well determined in order to predict the internal overpressure in the anodes. This parameter is known to be linked to internal cracks that can form in the anodes during baking.

As for the second objective of the paper (i.e., determine to what extent systematic thermogravimetric tests should be performed for modeling purposes when different raw materials are used in the anode composition, with potentially different kinetic parameters), the analysis could only provide "mixed answers". It is clear that some outputs are significantly affected by changes of the activation energies, while others are not. Depending on what one is looking for with the modeling and depending on the expected variance of the kinetic parameters, it might or might not be necessary to perform new measurements. However, at this point, no experimental data is available regarding the quantitative variability of the kinetic parameters. Furthermore, as mentioned above, some kinetic parameters are more important than others depending on which output is considered. That could influence the experimental setup.

It is worth mentioning that, according to the analysis, changes of kinetic parameters can affect the real operating baking furnace. Since, for most outputs of interest, linearity was satisfactory, it is possible to use eq 18 to predict the outputs of interest for a given set of inputs, as well as the variance of the outputs for given variances of the inputs.

8. CONCLUSIONS

The sensitivity analysis presented in this paper succeeded in explaining which kinetic parameters are the most influential on certain outputs of a detailed baking model including pitch pyrolysis. We used 3 techniques to analyze the sensitivity of chosen model outputs to the variation of the kinetic inputs. First, the calculation of the coefficient of variation allowed us to determine which outputs were significantly affected by the inputs, and which were not. Next, linear regression was used to gain more insights and to explain which of the 6 kinetic parameters are the most influential. Finally, a variance-based technique was used in order to explain the remaining variance of one output for which the linear regression did not give satisfactory results. The results showed that the activation energy of the 3 species (H_2, CH_4, and tar) should be well determined in order to predict accurately (i) the porosity evolution during baking, (ii) the heating value of the volatiles released in the flue channel of the baking furnace, and (iii) the maximum internal pressure in the anodes. The variance of these model outputs is of the order of the variance of the kinetic parameters. Therefore, model predictions can differ from reality if the variance of the kinetic parameters is important.

For future work, several new aspects should be considered:

- The third sensitivity analysis technique considered here required a lot of simulations in order to converge to coherent values and may not be suitable for 2D or 3D models requiring more CPU time. Other less time-consuming sensitivity analysis techniques should be considered.[54,57,58]
- In the present analysis, properties of all materials (e.g., conductivity, heat capacity) were kept the same for all the simulations. They were functions of temperature and porosity (so they evolved in time), but the correlation used to estimate them was considered as "certain". An interesting study would consist of quantifying how variability of these properties could affect the outputs of a detailed baking model. Similarly, the impact of variability of other input parameters, such as the percentage of pitch that will be pyrolyzed, could be looked at.
- The pyrolysis model considered three single step parallel reactions based on the Arrhenius equation. Other detailed approaches could be considered to represent more closely the actual phenomena that occur during baking. Sensitivity analysis could be used to determine which reactions are the most important for the outputs of interest.

AUTHOR INFORMATION

Corresponding Author

*E-mail: Louis.Gosselin@gmc.ulaval.ca. Tel.: +418-656-7829. Fax: +418-656-7415.

Notes

The authors declare no competing financial interest.

ACKNOWLEDGMENTS

The authors are grateful to the Natural Sciences and Engineering Research Council of Canada (NSERC) and to Alcoa for their financial support via an NSERC-Cooperative

Research and Development (RDC) grant entitled "Improvement of smelting energy efficiency through anode production improvement".

NOMENCLATURE

a = heating rate [K s^{-1}]
A_i = pre-exponential factor for species i [s^{-1}]
C = constants
E_i = activation energy for species i [J/mol]
K = permeability [m^2]
n_i = reaction order for species i
P = pressure [Pa]
R = molar gas constant [J mol^{-1} K^{-1}]
t = time [s]
T = temperature [K]
x = Cartesian coordinate [m]
X = random variable
$Y_{P,1}$ = model output representing maximal pressure achieved in the domain
$Y_{P,2}$ = model output representing time at which the peak pressure occurs
$Y_{HV,1}$ = model output representing maximum heating value flux
$Y_{HV,2}$ = model output representing time at which maximum heating value flux occurs
$Y_{\varepsilon,1}$ = model output representing time at which the average porosity of the anode is halfway between its initial and final values
$Y_{\varepsilon,2}$ = model output representing the maximum difference of porosity between anode surface and anode center that occurs during the baking

Greek Symbols

α = progress variable representing fraction of solids converted into gases
ε = porosity
μ = mean
ρ = density [kg m^{-3}]
σ = standard deviation
τ = final baking time [s]
χ = heating value [MJ·kg^{-1}]
ω = mass fraction

Subscripts

0 = initial
B = baked
G = green
i = species i
s = solid

REFERENCES

(1) Thonstad, J.; Fellner, P.; Haarberg, G.M.; Hives, J.; Kvande, H.; Sterten, A. *Aluminium Electrolysis: Fundamentals of the Hall-Héroult Process*; Aluminium-Verlag Marketing & Kommunikation GmbH: Düsseldorf, 2001.
(2) Hay, S. J.; Metson, J. B.; Hyland, M. M. Sulfur speciation in aluminum smelting anodes. *Ind. Eng. Chem. Res.* **2004**, *43* (7), 1690–1700.
(3) Furman, A.; Martirena, H. A mathematical model simulating an anode baking furnace. *Light Metals* **1980**, *1980*, 545–552.
(4) Hurlen, J.; Lid, O.; Naterstad, T.; Utne, P. Operation characteristics of a vertical flue ring furnace. *Light Metals* **1981**, *1981*, 569–581.
(5) de Fernandez, E.; Marletto, J.; Martirena, H. Combined mathematical simulation and experimental studies on a closed baking furnace. *Light Metals* **1983**, *1983*, 805–817.
(6) López Hercules, J. R.; Vargas Sarmiento, P. A. Mathematical model for a ring type anode baking furnace. *Light Metals* **1988**, *1988*, 315–323.
(7) Ordronneau, F.; Gendre, M.; Pomerleau, L.; Backhouse, N.; Berkovich, A.; Huang, X. Meeting the challenge of increasing anode baking furnace productivity. *Light Metals* **2011**, *2011*, 865–870.
(8) Keller, F.; Disselhorst, J. H. M. Modern anode bake furnace developments. *Light Metals* **1981**, *1981*, 611–621.
(9) Bui, R. T.; Charette, A.; Bourgeois, T. Simulating the process of carbon anode baking used in the aluminum industry. *Metall. Mater. Trans. B* **1984**, *15* (3), 487–492.
(10) Bui, R. T.; Charette, A.; Bourgeois, T. A computer model for the horizontal flue ring furnace. *IEEE Trans. Ind. Appl.* **1984**, *IA-20* (4), 894–901.
(11) Charette, A.; Bui, R. T.; Bourgeois, T. Modeling the heat transfer in a ring furnace. *IEEE Trans. Ind. Appl.* **1984**, *20* (4), 902–907.
(12) Bui, R. T.; Dernedde, E.; Charette, A.; Bourgeois, T. Mathematical simulation of a horizontal flue ring furnace. *Light Metals* **1984**, *1984*, 1033–1040.
(13) Thibault, M.; Bui, R. T.; Charette, A.; Dernedde, E. Simulating the dynamics of the anode baking ring furnace. *Light Metals* **1985**, *1985*, 1141–1151.
(14) Bui, R. T.; Charette, A.; Bourgeois, T.; Dernedde, E. Performance analysis of the ring furnace used for baking industrial carbon electrodes. *Can. J. Chem. Eng.* **1987**, *65* (1), 96–101.
(15) Bourgeois, T.; Bui, R. T.; Charette, A.; Sadler, B. Computer simulation of a vertical ring furnace. *Light Metals* **1990**, *1990*, 547–552.
(16) Ouellet, R.; Jiao, Q.; Chin, E.; Celik, C.; Lancaster, D.; Wilburn, D. Anode baking furnace modelling for process optimization. *Light Metals* **1995**, 653–662.
(17) Peter, S.; Charette, A.; Bui, R. T.; Tomsett, A.; Potocnik, V. An extended two-dimensional mathematical model of vertical ring furnaces. *Metall. Mater. Trans. B* **1996**, *27* (2), 297–304.
(18) Zhang, L. Q.; Zheng, C. G.; Xu, M. H. Simulating the heat transfer process of horizontal anode baking furnace. *Dev. Chem. Eng. Miner. Process.* **2005**, *13* (3–4), 447–458.
(19) Gundersen, Ø.; Balchen, J. G. Modeling and simulation of an anode carbon baking furnace. *Model., Identification Control* **1995**, *16* (1), 3–33.
(20) Bui, R. T.; Peter, S.; Charette, A.; Tomsett, A. D.; Potocnik, V. Modelling of heat transfer and gas flow in the vertical flue anode baking furnace. *Light Metals* **1995**, *1995*, 663–671.
(21) Jacobsen, M.; Melaaen, M. C. Heat and mass transfer in anode materials during baking. *Light Metals* **1995**, *1995*, 681–690.
(22) Kocaefe, Y. S.; Dernedde, E.; Kocaefe, D.; Ouellet, R.; Jiao, Q.; Crowell., W. F. A 3d mathematical model for the horizontal anode baking furnace. *Light Metals* **1996**, *1996*, 529–534.
(23) Jacobsen, M.; Melaaen, M. C. Numerical simulation of the baking of porous anode carbon in a vertical flue ring furnace. *Numer. Heat Transfer, Part A: Appl.* **1998**, *34* (6), 571–598.
(24) Severo, D. S.; Gusberti, V.; Pinto, E. C. V. Advanced 3d modelling for anode baking furnaces. *Light Metals* **2005**, *2005*, 697–702.
(25) Hulse, K. L. *Anode Manufacture: Raw Materials Formulation and Processing Parameters*; R&D Carbon Ltd., 2000.
(26) Meier, M. W. *Cracking: Cracking Behaviour of Anodes*; R&D Carbon Ltd., 1996.
(27) Zander, M. On the composition of pitches. *Fuel* **1987**, *66* (11), 1536–1539.
(28) Martnez-Alonso, A.; Bermejo, J.; Tascón, J. M. D. Thermoanalytical studies of pitch pyrolysis. *J. Therm. Anal. Calorim.* **1992**, *38* (4), 811–819.

(29) Martnez-Alonso, A.; Bermejo, J.; Granda, M.; Tascón, J. Suitability of thermogravimetry and differential thermal analysis techniques for characterization of pitches. *Fuel* **1992**, *71* (6), 611−617.
(30) Gundersen., Ø. *Modelling of Structure and Properties of Soft Carbons with Application to Carbon Anode Baking*. PhD thesis, Norwegian University of Science and Technology (NTNU), 1998.
(31) Dernedde, E.; Charette, A.; Bourgeois, T.; Castonguay, L. Kinetic phenomena of the volatiles in ring furnaces. *Light Metals* **1986**, *1986* (2), 589−592.
(32) Tremblay, F.; Charette, A. Cinétique de dégagement des matières volatiles lors de la pyrolyse d'électrodes de carbone industrielles. *Can. J. Chem. Eng.* **1988**, *66*, 86−96.
(33) Charette, A.; Kocaefe, D.; Saint-Romain, J. L.; Couderc, P. Comparison of various pitches for impregnation in carbon electrodes. *Carbon* **1991**, *29* (7), 1015−1024.
(34) Slovák, V.; Šušák, P. Pitch pyrolysis kinetics from single tg curve. *J. Anal. Appl. Pyrolysis* **2004**, *72* (2), 249−252.
(35) Yue, C.; Watkinson, A. P. Pyrolysis of pitch. *Fuel* **1998**, *77* (7), 695−711.
(36) Carrasco., F. The evaluation of kinetic parameters from thermogravimetric data: Comparison between established methods and the general analytical equation. *Thermochim. Acta* **1993**, *213*, 115−134.
(37) Galwey, A. K. Is the science of thermal analysis kinetics based on solid foundations?: A literature appraisal. *Thermochim. Acta* **2004**, *413* (1), 139−183.
(38) Marcilla, A.; Gomez, A.; Menargues, S.; Garcia-Quesada., J. C. New approach to elucidate compensation effect between kinetic parameters in thermogravimetric data. *Ind. Eng. Chem. Res.* **2007**, *46* (13), 4382−4389.
(39) Tremblay, F. *Cinétique de dégagement des matières volatiles lors de la pyrolyse d'électrodes de carbones industrielles*. Master's thesis, Université du Québec à Chicoutimi (UQAC), 1988.
(40) Edwards, L. C.; Neyrey, K. J.; Lossius., L. P. A review of coke and anode desulfurization. *Light Metals* **2007**, *2007*, 895−900.
(41) Mannweiler, U.; Fischer, W. K.; Perruchoud, R. C. Carbon products: A major concern to aluminum smelters; www.rd-carbon.com, 2009.
(42) Maroto-Valer, M. M.; Zhang, Y.; Shaffer, B. N.; Andrésen, J. M. Pyrolysis yields of coal tar pitches: Effect of polymerization additives. *Fuel Chem. Div. Prepr.* **2002**, *47* (1), 185−186.
(43) Bouchard, N. *Pyrolyse de divers brais utilisés dans la technologie Söderberg et analyse des matières volatiles*. Master's thesis, Université du Québec à Chicoutimi (UQAC), 1998.
(44) Wilke, C. R. Diffusional properties of multicomponent gases. *Chem. Eng. Prog. (CEP)* **1950**, *46* (2), 96−104.
(45) Babu, B. V.; Chaurasia, A. S. Dominant design variables in pyrolysis of biomass particles of different geometries in thermally thick regime. *Chem. Eng. Sci.* **2004**, *59* (3), 611−622.
(46) Hagge, M. J.; Bryden, K. M. Modeling the impact of shrinkage on the pyrolysis of dry biomass. *Chem. Eng. Sci.* **2002**, *57* (14), 2811−2823.
(47) Sadhukhan, A. K.; Gupta, P.; Saha, R. K. Modelling of pyrolysis of large wood particles. *Bioresour. Technol.* **2009**, *100* (12), 3134−3139.
(48) Thibault, M.-A. *Modèle dynamique du four de cuisson d'anodes*. Master's thesis, Université du Québec à Chicoutimi (UQAC), 1984.
(49) Sverdlin, V. A.; Priezzhaya, L. A.; Yanko, E. A. Study of kinetics of thermal transformation of carbon anodes for aluminium electrolysis. *Light Metals* **1991**, *1991*, 673−678.
(50) *Comsol Multiphysics Reference Guide Version 4.2a*; Comsol Inc: Burlington, MA, 2011.
(51) Holdner, D. N.; Nadkarni, S. K.; DuTremblay, D. Evaluation of the uniformity of baking in horizontal and vertical flue ring furnaces. *Light Metals* **1983**, *1983*, 797−804.
(52) Keller, F.; Sulger, P. O. *Anode Baking - Baking of Anodes for the Aluminum Industry*; R&D Carbon Ltd., 2008.
(53) Lustenberger, M. *Heat Treatment of Carbon Anodes for the Aluminium Industry*. PhD thesis, École Polytechnique Fédérale de Lausanne (EPFL), 2004.
(54) Saltelli, A.; Ratto, M.; Andres, T.; Campolongo, F.; Cariboni, J.; Gatelli, D.; Saisana, M.; Tarantola, S. *Global Sensitivity Analysis: The Primer*; John Wiley & Sons: Hoboken, NJ, 2008.
(55) Maiwald, D.; Lisa, D. D.; Mnikoleiski, H. P. Full control of pitch burn during baking: It's impact on anode quality, operational safety, maintenance and operational costs. *Light Metals* **2011**, *2011*, 875−880.
(56) Plischke, E. An effective algorithm for computing global sensitivity indices (easi). *Reliab. Eng. Syst. Saf.* **2010**, *95* (4), 354−360.
(57) Li, G.; Wang, S. W.; Rabitz, H.; Wang, S.; Jaffé, P. Global uncertainty assessments by high dimensional model representations (HDMR). *Chem. Eng. Sci.* **2002**, *57* (21), 4445−4460.
(58) Franceschini, G.; Macchietto, S. Model-based design of experiments for parameter precision: State of the art. *Chem. Eng. Sci.* **2008**, *63* (19), 4846−4872.